ChemPhotoChem

Research Articles
doi.org/10.1002/cptc.202200057

Chemistry Europe
European Chemical Societies Publishing

www.chemphotochem.org

Electronic Circular Dichroism Unravels Atropisomers of a Broadly Absorbing Fulgide Derivative

Volker Hermanns,[a] Maximilian Scheurer,[b] Andreas Dreuw,*[b] Josef Wachtveitl,*[c] Markus Braun,*[c] and Alexander Heckel*[a]

We prepared and studied six atropisomers with different chiroptical properties emerging from a single, robust, broadly-absorbing fulgide photoswitch. After separation of the different atropisomers via HPLC on a chiral column, their isomerization processes at room temperature and the energy barriers of the different species were investigated in detail using spectroscopic and theoretical methods.

Introduction

Photoactivatable compounds such as photolabile protecting groups (photocages) and photoswitches are widely used for achieving light control in different research areas.[1,2] Some of the best explored photoswitches e.g. stilbene, azobenzene, spiropyran and fulgide or fulgimide are already applied in biological studies.[3] Reversible photoswitching enables turning (biological) activity ON and OFF. Due to its broad absorption range, thermal stability, and robust photochemistry, the fulgide photoswitch is an ideal photochemical tool.[4,5] The trifluoromethyl-substituted derivative developed by Yokoyama and Takahashi,[6] can be switched photochemically between three different isomers at different wavelengths (Figure 1). The (*E*)-isomer (open minor form) can be accumulated from the (*Z*)-isomer (open major form) at 365 nm. A photochemically allowed, thermally forbidden pericyclic reaction of the (*Z*)-isomer results in the (*C*)-isomer (closed form) at 430 nm, which is thermally stable. Besides synthetic modifications in previous studies which optimized the photostability,[7,8] many spectroscopic studies improved the understanding of the photochemical processes of the fulgide scaffold.[9–20]

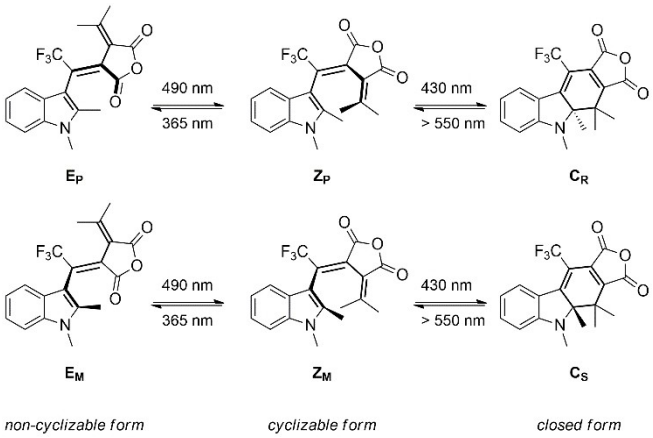

Figure 1. The six isomeric forms of the fulgide photoswitch. There are three different photoisomeric forms with two enantiomers each.

Up to now there are only few studies on the different atropisomers of these species.[21,22] A rotation between the C3 of the indolyl part and the adjacent carbon atom should be possible. Yet, most of the existing studies do not take the different atropisomers into account. In this study, we observed that there is a rotation barrier, which arises from the steric hindrance of the 6-membered benzenic ring of the indolyl part. This observation is supported by theoretical calculations. Both the carbonyl-oxygen of the (*E*)-isomer and the isopropylidene-group of the (*Z*)-isomer should in principle interfere with the benzenic ring and with the methyl group at the 2-position of the indolyl part. The differences between the two enantiomers of the (*C*)-isomer are much more subtle. Upon ring-opening, a helical molecular structure with right- or left-handed helicity is formed which is based on the photochromic cyclohexadiene/hexatriene motif. Thus, the ring-opening/ring-closure reaction has a very significant effect on the helicity of the fulgide compound.

[a] *V. Hermanns, Prof. Dr. A. Heckel*
Institute for Organic Chemistry and Chemical Biology
Goethe-University Frankfurt
Max-von-Laue Str. 9, 60438 Frankfurt (Germany)
E-mail: heckel@uni-frankfurt.de
[b] *Dr. M. Scheurer, Prof. Dr. A. Dreuw*
Interdisciplinary Center for Scientific Computing
Heidelberg University
Im Neuenheimer Feld 205, 69120 Heidelberg (Germany)
E-mail: dreuw@uni-heidelberg.de
[c] *Prof. Dr. J. Wachtveitl, Dr. M. Braun*
Institute of Physical and Theoretical Chemistry
Goethe-University Frankfurt
Max-von-Laue Str. 9, 60438 Frankfurt (Germany)
E-mail: wveitl@theochem.uni-frankfurt.de
braun@theochem.uni-frankfurt.de

Supporting information for this article is available on the WWW under https://doi.org/10.1002/cptc.202200057

Results and Discussion

The thermally robust fulgide derivative was synthesized as described in the literature.[23] A first hint for the different chemical context of the methyl groups of the respective compounds could be observed via 1H-NMR as all four methyl group signals of the indole part of the two (*E*)-isomers show a downfield shift compared to the (*Z*)-isomer. Also the individual methyl groups at the isopropylidene substituent show different chemical shifts (see Supporting Information).

With these observations, we wanted to take a closer look at the individual atropisomers (Figure 1). The stereodescriptors were assigned applying the rules of ref. [24] to the single bond in the 3-position of the indolyl ring. To obtain the different (*M*)- and (*P*)- atropisomers of the respective fulgide derivatives, we used reverse-phase chiral column chromatography to separate the different species (Figure 2). When we finally found out the optimal solvent mixture, we observed two different, nearly baseline- separated peaks for compounds $\mathbf{Z_M}$ and $\mathbf{Z_P}$ and also for $\mathbf{E_M}$ and $\mathbf{E_P}$ (Figure 2). As the difference between the $\mathbf{C_R}$ and $\mathbf{C_S}$ isomers are very subtle, they could not be separated directly by chromatography on the chiral column. However, the absorption bands of the (*C*)-isomers are perfectly separated from the (*Z*)- and (*E*)-isomers and the conversion is very clean. Therefore, by irradiation of $\mathbf{Z_M}$ and $\mathbf{Z_P}$ at 430 nm, we were finally able to obtain $\mathbf{C_S}$ and $\mathbf{C_R}$, respectively.

The UV/vis spectra of each of the compounds were in accord with previous literature (Figure 2b). After the separation, it was now possible to study the ECD spectra of the different isomers separately. Toluene was chosen because it is the solvent in which the fulgide photoswitch is most often used. Importantly, fulgide photoswitching was investigated in different solvents before[14] and the use of toluene resulted in higher quantum yields and smaller barriers in the excited states for the ring-opening reaction compared to for example acetonitrile. The ECD spectra of the corresponding atropisomers show the expected symmetry to the wavelength axis (Figure 3).

With all six atropisomers in hand, we investigated the thermal stability of each isomer. We therefore performed thermal racemization experiments under light exclusion and plotted the decaying ECD response at different temperatures (Figure 4). The evaluation was performed in the indicated time windows. We verified that the racemization occurs completely without remaining offset signal. As expected, the C-atropisom-

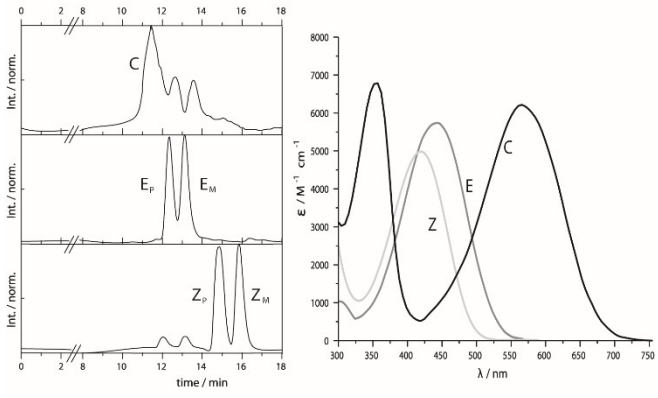

Figure 2. Left: Preparative HPLC separation (isocratic 85% n-hexane/15% ethanol) of the three species on a chiral support. (Daicel™ CHIRALPAK® 1 A, 5 µm, 20 mm×250 mm, flowrate: 18 mL/min). Top: (*C*)-isomers with residual (*E*)-isomers after irradiation at 430 nm (λ_{detec} = 590 nm). Middle: (*E*)-isomers after accumulation by irradiation at 365 nm (λ_{detec} = 430 nm). Bottom: (*Z*)-isomers as obtained in the initial synthesis with a small amount of (*E*)-isomers (λ_{detec} = 420 nm). Right: The molar absorption coefficient of the respective photoisomers.

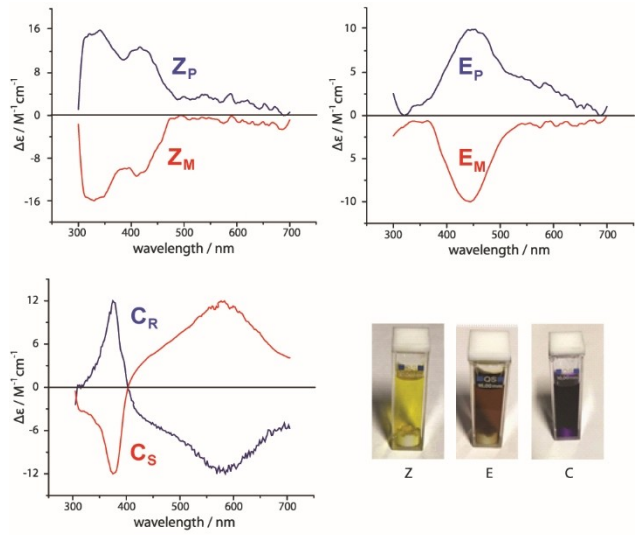

Figure 3. ECD spectra and pictures of the solutions of the corresponding atropisomers dissolved in toluene, measured at room temperature.

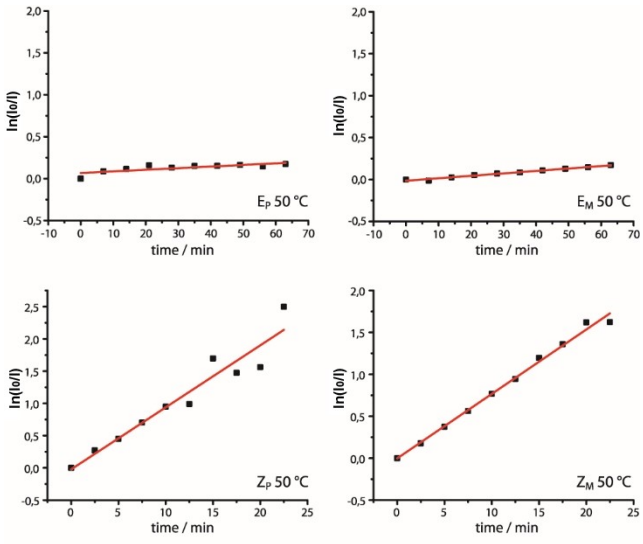

Figure 4. Thermal racemization for the different (*E*)- and (*Z*)-isomers at 50 °C. Measurements at 35 °C and 70 °C are shown in the Supporting Information. ECD spectra were recorded during constant temperature and under light exclusion. The y-axis shows the integral over the respective ECD curves at the indicated times referenced to the one at the start of the investigation on a logarithmic scale – indicative for the enantiomeric excess. All measurements were performed in toluene.

ers showed no significant thermal racemization up to 70 °C, as their rotation is locked through cyclisation (Table 1). When comparing the (*E*)- and the (*Z*)-atropisomers, we observed that the (*E*)-atropisomers showed significantly higher thermal stability and were nearly stable up to 50 °C. Still, the two (*Z*)-atropisomers were relatively stable below 35 °C which also allows the use of this system for application at room temperature or below. The photochemical and thermal properties of all atropisomers are summarized in Table 1. Our experimental data resulted in an energy difference of the rotational barriers of about 2 kcal/mol for the transition between $\mathbf{E_M}$ and $\mathbf{E_P}$ and for $\mathbf{Z_M}$ and $\mathbf{Z_P}$, which fits well to similar rotational barriers in the literature.[25]

To compare our experimental results and for the assignment of the different atropisomers, theoretical calculations were performed. A relaxed potential energy surface (PES) scan for the torsion angle between the indole moiety and the isopropylidene substituent using CAM–B3LYP/def2-SVP for (*E*)- and (*Z*)-isomers is shown in Figure 5.

Computational details can be found in the Supporting Information. For the (*E*)-isomer, two distinct barriers for the rotation are identified at 0° and 180°, i.e. when the carbonyl group is coplanar with the indole moiety. The energy profile of the (*Z*)-isomer also possesses these two high-energy barriers, however, due to the isopropylidene group passing the indole moiety during rotation around the dihedral, two distinct minima are found on each side of the 0° barrier. For the (*E*)-isomer, these regions of the PES are quite flat with several local minima. Nonetheless, the PES scans illustrate the differing properties of (*E*)- and (*Z*)-isomers for the interconversion between their respective atropisomers. Also, compared to the experimentally observed barriers for the rotation, the same trend of the computed barriers is observed with the one for the (*E*)-isomer being higher than the one for the (*Z*)-isomer. The discrepancy between the experimentally and computationally determined barrier heights falls well within the expected error of the computational approach.

From the PES scan snapshots as the starting point, we could also obtain fully optimized geometries for the atropisomers to correctly assign the experimental ECD spectra in Figure 3.

As these results led already to a clearer view about the thermal and rotational properties of each atropisomers, we tested whether the ECD-spectra and therefore the stereochemical information stays intact upon photoswitching between the different photoisomers (*Z*)-(*C*) and (*E*)-(*Z*). Photoswitching between (*Z*)- and (*C*)-isomers at 20 °C showed, that a significant difference between the corresponding isomers can be observed for more than 10 switching cycles (Figure 6). This behavior shows again the robust photochemistry of the switching process between these two isomers. Photoswitching between the (*Z*)- and the (*E*)-isomer of the fulgide derivative turned out to be more complex than (*Z*)-(*C*) photoswitching, as also described in literature. As irradiation of the (*Z*)-isomer at 365 nm for switching from (*Z*) to (*E*) results not only in the (*E*)-form, the behavior was not as clear as for the (*Z*)-(*C*)-switching. Upon irradiation of the (*Z*)-isomers with light at 365 nm there is also some conversion to the (*C*)-isomer because of the overlapping absorption bands.

Figure 7 summarizes our results. The color of the (*E*)-isomers after separation, dissolved in toluene turned out to be brownish. The thermal racemization between $\mathbf{E_M}$ and $\mathbf{E_P}$ at room temperature is very slow with a high energy barrier of about 23 kcal/mol. Both atropisomers show only one characteristic ECD signal. Photoswitching to the respective (*Z*)-isomer can be performed by irradiation with 490 nm.

The (*Z*)-isomer shows a yellow color when dissolved in toluene. It can be switched to either the (*E*)- or the (*C*)-photoisomers with 365 nm or 430 nm, respectively. It shows two characteristic peaks in the ECD spectrum and only slow thermal racemization between $\mathbf{Z_P}$ and $\mathbf{Z_M}$ at ambient temperatures. $\mathbf{C_R}$ and $\mathbf{C_S}$ do not thermally racemize directly. These isomers are dark violet, when dissolved in toluene and have a high extinction coefficient. The ECD signal shows two characteristic signals (at 365 nm and 580 nm) of opposite sign.

Table 1. Photochemical and thermal properties of the different atropisomers.[a]

Experimental data Compd.	λ_{max} [nm]	$k_{(35\,°C)}$ [s^{-1}]	$k_{(50\,°C)}$ [s^{-1}]	$k_{(70\,°C)}$ [s^{-1}]	ΔG [kcal/mol]
$\mathbf{1E_M}$	447	n.obs.	0.0019	0.0193	23/22.9
$\mathbf{1E_P}$	447	n.obs.	0.0029	0.0250	22.7/22.7
$\mathbf{1Z_M}$	427	0.0123	0.0962	n.d.	20.7/20.5
$\mathbf{1Z_P}$	427	0.0129	0.0769	n.d.	20.7/20.6
$\mathbf{1C_R}$	572	n.obs.	n.obs.	n.obs.	n.d.
$\mathbf{1C_S}$	572	n.obs.	n.obs.	n.obs.	n.d.

[a] All measurements were performed in toluene. n.d. means not determined. n.obs. means $k < 0.0001$.

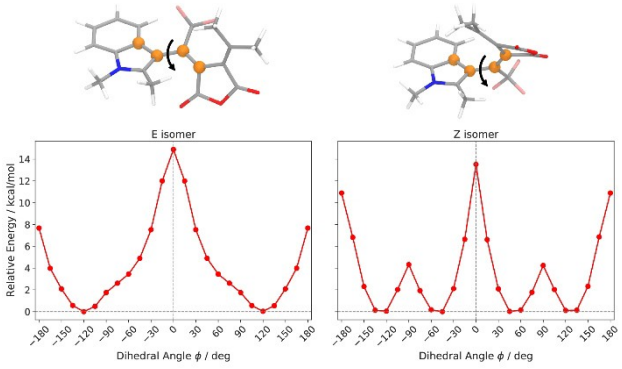

Figure 5. Relaxed potential energy surface scan along the dihedral angle connecting the indole moiety and the isopropylidene moiety. Constraint optimizations were run at the CAM–B3LYP/def2-SVP level of theory. The (*E*)- and (*Z*)-isomers ($\phi(E) = -165\,°$ and $\phi(Z) = 120\,°$) are illustrated above the respective energy plot, and the four atoms defining the dihedral angle are highlighted in orange. The direction of rotation (increasing dihedral angle) are indicated by arrows. Energies are relative to the minimum energy found in the respective scan.

Conclusion

In summary, we identified all atropisomers of the described thermal robust fulgide derivative and determined the rotational

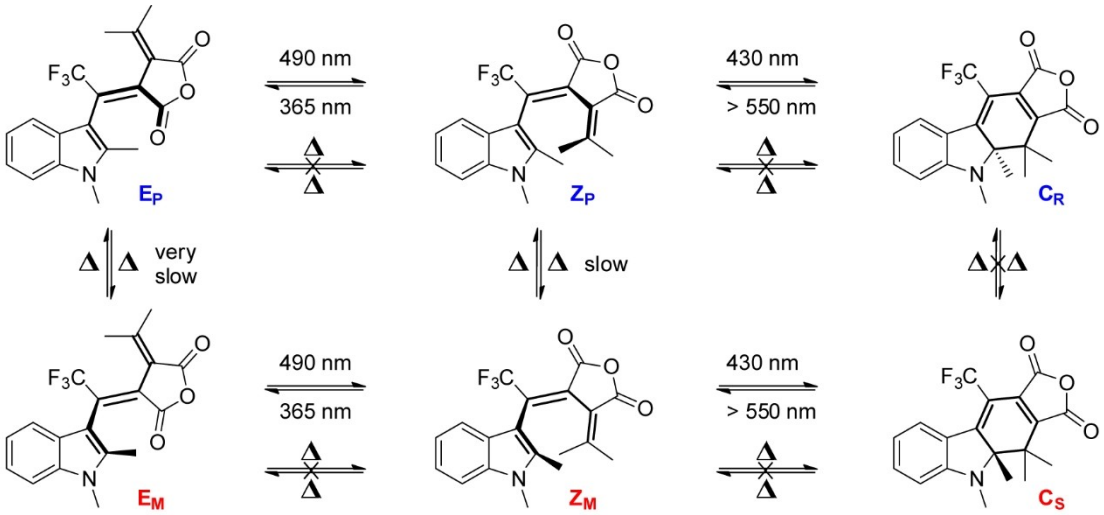

Figure 6. Photoswitching cycles upon repetitive irradiation of Z_P (a) and Z_M (b) in toluene at 430 nm and 550 nm.

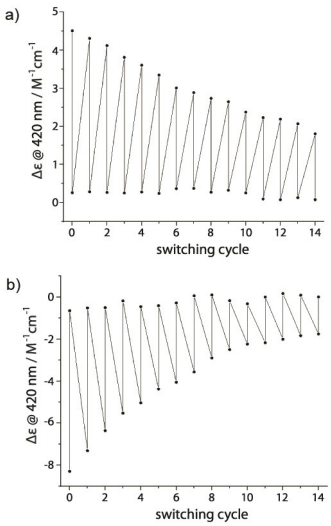

Figure 7. Atropisomers of the fulgide derivative. Photoisomerization can be done between the *E* and the *Z* or between the *Z* and the *C* form, when choosing the right wavelength. The thermal isomerization rates were determined via CD spectroscopy and compared with the energy barrier values from the computational calculations. The assignment of the isomers (blue/red) to the right ECD-spectrum (blue/red) was performed with computational methods.

barriers of the (Z_M), (Z_P), (E_M) and (E_P)-isomers with experimental and theoretical methods. Additionally ECD spectra of all six isomers, which are complementary across the whole spectrum, are presented.

Acknowledgements

This work was supported by the Deutsche Forschungsgemeinschaft (DFG) through the research training group "CLiC" (GRK 1986, Complex Light Control). We thank Oliver Pereira and Trinetri Goel for their help. Open Access funding enabled and organized by Projekt DEAL.

Conflict of Interest

The authors declare no conflict of interest.

Data Availability Statement

The data that support the findings of this study are available in the supplementary material of this article.

Keywords: atropisomers · circular dichroism · energy barriers · fulgide · photoswitch

[1] R. Weinstain, T. Slanina, D. Kand, R. Klán, *Chem. Rev.* **2020**, *120*, 13135–13272.
[2] M. Kathan, S. Hecht, *Chem. Soc. Rev.* **2017**, *46*, 5536–5550.
[3] W. Szymański, J. M. Beierle, H. A. V. Kistemaker, W. A. Velema, B. L. Feringa, *Chem. Rev.* **2013**, *113*, 6114–6178.
[4] M. Reinfelds, V. Hermanns, T. Halbritter, J. Wachtveitl, M. Braun, T. Slanina, A. Heckel, *ChemPhotoChem* **2019**, *3*, 441–449.
[5] I. B. Ramsteiner, A. Hartschuh, H. Port, *Chem. Phys. Lett.* **2001**, *343*, 83–90.
[6] Y. Yokoyama, K. Takahashi, *Chem. Lett.* **1996**, *25*, 1037–1038.
[7] M. A. Wolak, N. B. Gillespie, C. J. Thomas, R. R. Birge, W. J. Lees, *J. Photochem. Photobiol. A* **2001**, *144*, 83–91.
[8] N. I. Islamova, X. Chen, S. P. Garcia, G. Guez, Y. Silva, W. J. Lees, *J. Photochem. Photobiol. A* **2008**, *195*, 228–234.
[9] M. A. Wolak, J. M. Sullivan, C. J. Thomas, R. C. Finn, R. R. Birge, W. J. Lees, *J. Org. Chem.* **2001**, *66*, 4739–4741.
[10] M. A. Wolak, C. J. Thomas, N. B. Gillespie, R. R. Birge, W. J. Lees, *J. Org. Chem.* **2003**, *68*, 319–326.
[11] S. Malkmus, F. O. Koller, S. Draxler, T. E. Schrader, W. J. Schreier, T. Brust, J. A. DiGirolamo, W. J. Lees, W. Zinth, M. Braun, *Adv. Funct. Mater.* **2007**, *17*, 3657–3662.
[12] T. Cordes, S. Malkmus, J. A. DiGirolamo, W. J. Lees, A. Nenov, R. de Vivie-Riedle, M. Braun, W. Zinth, *J. Phys. Chem. A* **2008**, *112*, 13364–13371.
[13] T. Brust, S. Draxler, S. Malkmus, C. Schulz, M. Zastrow, K. Rück-Braun, W. Zinth, M. Braun, *J. Mol. Liq.* **2008**, *141*, 137–139.
[14] T. Brust, S. Malkmus, S. Draxler, S. A. Ahmed, K. Rück-Braun, W. Zinth, M. Braun, *J. Photochem. Photobiol. A* **2009**, *207*, 209–216.
[15] S. Draxler, T. Brust, S. Malkmus, J. A. DiGirolamo, W. J. Lees, W. Zinth, M. Braun, *Phys. Chem. Chem. Phys.* **2009**, *11*, 5019–5027.

[16] T. Brust, S. Draxler, A. Popp, X. Chen, W. J. Lees, W. Zinth, M. Braun, *Chem. Phys. Lett.* **2009**, *477*, 298–303.
[17] T. Cordes, T. T. Herzog, S. Malkmus, S. Draxler, T. Brust, J. A. DiGirolamo, W. J. Lees, M. Braun, *Photochem. Photobiol. Sci.* **2009**, *8*, 528–534.
[18] T. Brust, S. Draxler, J. Eicher, W. J. Lees, K. Rück-Braun, W. Zinth, M. Braun, *Chem. Phys. Lett.* **2010**, *489*, 175–180.
[19] A. Nenov, W. J. Schreier, F. O. Koller, M. Braun, R. de Vivie-Riedle, W. Zinth, I. Pugliesi, *J. Phys. Chem. A* **2012**, *116*, 10518–10528.
[20] C. Slavov, N. Bellakbil, J. Wahl, K. Mayer, K. Rück-Braun, I. Burghardt, J. Wachtveitl, M. Braun, *Phys. Chem. Chem. Phys.* **2015**, *17*, 14045–14053.
[21] Y. Yokoyama, Y. Shimizu, S. Uchida, Y. Yokoyama, *J. Chem. Soc. Chem. Commun.* **1995**, *7*, 785–786.
[22] C. Petermayer, H. Dube, *J. Am. Chem. Soc.* **2018**, *140*, 13558–13561.
[23] C. J. Thomas, M. A. Wolak, R. R. Birge, W. J. Lees, *J. Org. Chem.* **2001**, *66*, 1914–1918.
[24] G. P. Moss, *Pure Appl. Chem.* **1996**, *68*, 2193–2222.
[25] Y. Yokoyama, *Chem. Rev.* **2000**, *100*, 11717–1739.

Manuscript received: March 2, 2022
Revised manuscript received: April 30, 2022
Accepted manuscript online: May 3, 2022
Version of record online: May 31, 2022